Risk Analysis of Earthquake-Induced Submarine Slope Failure

Rafael RODRÍGUEZ-OCHOA [a], Farrokh NADIM [b] and José M. CEPEDA [b]

[a] *Department of Geosciences, University of Oslo, Norway*
[b] *Norwegian Geotechnical Institute (NGI), Norway*

Abstract. This paper presents an offshore risk analysis in a systematic manner to assess the influence of earthquake-induced submarine slope failure on offshore structures. The risk analysis is carried out for the future development of a natural gas field in deep waters in the south part of the Gulf of Mexico. The study accounts for all the elements in the conventional risk formulation: *Risk = Hazard × Consequences*. The hazard analysis was performed in two steps: first estimating the probability of earthquake-induced slope failure by using the slope failure fragility curve approach; and second estimating the probability of failed sediments impacting offshore structures by running debris flow numerical simulations in a Monte Carlo method framework. The consequences were estimated focused solely on the damage to offshore structures, in monetary terms, and the development of vulnerability curves as function of the velocity and the thickness of the moving mud flow that may evolve from the failed sediments.

Keywords. offshore geohazards, earthquakes, submarine landslides, risk analysis

1. Introduction

The failure of submarine slopes on the continental shelf and/or continental slope poses a risk to offshore structures and facilities from diverse economic sectors. The oil and gas industry is especially concerned about this natural phenomenon due to its increasing interest in developing gas and oil fields in deep waters, which involves the deployment of seabed installations and equipment on the continental slope.

This paper presents an assessment risk analysis of earthquake-induced submarine slope failure for a future gas field development in deep waters in the south part of the Gulf of Mexico. The risk analysis is approached in a systematic manner, first accounting for the hazard by using the slope failure fragility curve approach developed by Rodríguez-Ochoa et al. (2015b), and then debris flow numerical simulations using the BING code (Imran, 2001a) in a Monte Carlo framework. The consequences were quantified by identifying the elements at risk and assessing their vulnerability curves.

The analysis focused on the direct consequences related to the damage of offshore structures.

2. Site Characterization

The submarine slope under study is located in the south of the Gulf of Mexico, in the transition zone of the continental shelf to the continental slope, with water depth of about 500 m (Figure 1).

This slope is one of the nine potential unstable slopes identified by Fugro (2009) during the geophysical explorations. The largest slope angle of all the nine identified slopes is about 9.2 degrees. This submarine slope was modelled as a composite slope, the first part has 10 degrees with 600m horizontal distance and the second part has 5 degrees with 400m horizontal distance.

The sediments are cohesive calcareous soils with carbonate content between 11 to 23% and are classified as high plasticity clays.

Laboratory soil sensitivity varies from 3 to 5 down to 20m depth and from 1.5 to 3 beneath 20m. The estimated overconsolidation ratios (OCR) indicate that the sediments are normally consolidated to slightly overconsolidated.

The seismicity of the region is of concern. The site is influenced by the subduction zone in the Pacific coast, nearby volcanos, and the transform zone in the Caribbean Sea. The main risk posed to the marine environment and the

planned natural gas production facilities on the seabed is considered to be due to submarine landslides trigger by earthquakes. For further information see Rodríguez-Ochoa et al. (2015c).

Figure 1. Location of the submarine slope under study.

3. Slope Failure Hazard Analysis

The main objective of the earthquake-induced slope failure hazard analysis is to estimate the annual probability of slope failure. One of the few methods available to estimate the slope failure hazard due to a seismic event was developed by Nadim (2012), and refined by Rodríguez-Ochoa et al. (2015b). The procedure follows a probabilistic framework comprising various mathematical methods including Monte Carlo simulation, Bayesian inference and First Order Reliability Method (FORM).

The philosophy of the updated method is to estimate the unconditional annual probability of slope failure based on fragility curves. The slope failure fragility curves are obtained by performing dynamic analyses to assess the seismic slope stability based on the induced shear strains in the clay layers. The input motions are obtained from a probabilistic seismic hazard analysis (PSHA) in the site to estimate the probable earthquakes that may strike the site. For this study four strong motions with return periods of 1000, 5000, 10,000 and 100,000 were recommended (Geomatrix, 2006).

Once the fragility curves are determined, the mathematical expectation operator is applied to the estimated seismic hazard function and the estimated fragility slope failure function, normalized with respect to the return period, to obtain the annual probability of slope failure; by summing the products of the probability of each event (Seismic Hazard Function) by the value of that event (Normalized Fragility Slope Failure Function).

After applying the proposed methodology, the unconditional annual probability of earthquake-induced slope failure was estimated to be $1.2 \cdot 10^{-3}$.

4. Mud Flow Impact Hazard Analysis

4.1. BING Computer Code

To estimate the probability of mud flow impacting downslope offshore installations once the slope has failed, the computer code BING (Imran et al. 2001a) was used. BING is a 1-D numerical model that simulates the downslope spreading of a submarine debris flow. BING is able to use three different rheological models: Bingham, Herschel-Bulkley, and Bilinear. The main outcomes of BING are the runout distance, front velocity, and the final shape of the failed sediments.

In this study, the Bilinear rheological model was used for the numerical simulations with BING. This model has shown to give acceptable results in previous studies (Locat, 1997; Imran et al. 2001b; Jeong et al. 2010).

The bilinear model proposed by Locat (1997) has been adapted for numerical modelling by Imran et al. (2001a) as shown in Eqs. (1), (2) and (3).

$$\frac{\tau}{\tau_{ya}} = 1 + \frac{\gamma}{\gamma_r} - \frac{1}{1 + r\frac{\gamma}{\gamma_r}} \tag{1}$$

$$\gamma_r = \frac{\tau_{ya}}{\mu_{dh}} \tag{2}$$

$$r = \frac{\gamma_r}{\gamma_0} \tag{3}$$

where:
τ = shear stress (Pa);
γ = shear strain rate (s^{-1});
γ_r = reference strain rate (s^{-1});
r = ratio of strain rates;
τ_{ya} = apparent yield strength (Pa);

μ_{dh} = viscosity at high shear strain rates (plastic viscosity) (Pa.s);

γ_0 = shear strain rate at the transition from a Newtonian to a Bingham behaviour (s^{-1}).

4.2. Monte Carlo Simulation of Runout Scenarios

To quantify the effect of uncertainty in the BING input parameters on the runout distance, the Monte Carlo simulation method was used to obtain the probability distribution function of the runout distance.

The random variables used in the Monte Carlo simulations, with their range of values and proposed probability distributions are listed in Table 1. The means (μ) of the distribution functions were calculated by assuming symmetric normal distribution functions, and the standard deviations (σ) by using the following approximation: $\sigma = (max-min)/6$.

Table 1. Random variables

Variable	Mean, Std or Range	Probability Function
ρ_{mud} (kg/m^3)	1337, 29	Normal
τ_{ya} (Pa)	353, 100	Normal
γ_r (1/s)	1039, 52	Normal
r	6414, 1843	Normal
Initial Geometry	1 and 2	Discrete Uniform

The above input parameters are the mud density (ρ_{mud}), apparent yield strength (τ_{ya}), reference shear strain (γ_r), ratio of strain rates (r), and initial geometry configuration.

The range of values for the mud density as well as the parameters of the Bilinear rheological model (τ_{ya}, γ_r and r) were set based on the water content of the flowing mass and the empirical correlations developed by Locat (1997).

Regarding the random variable identified as Initial Geometry, this variable accounts for the initial geometry configuration of the failed sediments. BING assumes by default that the initial geometry of the debris mass has a parabolic shape.

To run the numerical simulations it was proposed to use two initial geometry configurations:

1. Configuration No.1 matches the initial length of the estimated slide surface with the initial length of mud deposit (i.e. base of the parabola = 600m), and a maximum thickness of mud deposit of 12m.

2. Configuration No.2 matches the initial thickness of the slide surface with the maximum thickness of the mud deposit (i.e. height of the parabola = 8m), and an initial length of mud deposit of 900m.

In the Monte Carlo simulations, 100 values for each random variable were generated using the specified ranges and probability distribution functions shown in Table 1. The stratified Latin Hyper Cube sampling technique proposed by McKay et al. (2000) was used to ensure a good representation of the distribution functions for all the random variables.

4.3. Runout Distance

Figure 2 shows the expected runout route down-slope of the failed sediments. This route goes along a natural channel that was formed due to previous slide activities and mass gravity flows which eroded the seafloor along the continental slope. Therefore, the topographic profile along the natural channel was used in BING to run the numerical simulations.
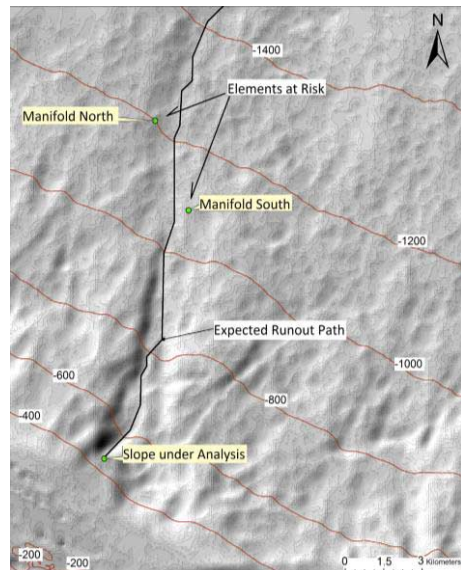

Figure 2. Expected runout path of the failed sediments, and location of source and exposed elements for the risk analysis.

Figure 3 shows the cumulative distribution functions generated to fit the numerically

simulated runout distances. It can be observed that the lognormal distribution fits well the data. The mean and standard deviation of the fitted distribution were 9.97 km and 2.83 km respectively. This probability distribution was used to estimate the probability of a mud flow with potential to damage offshore structures reaching specific locations along the channel. The case study focused on two manifolds that will be deployed to develop the natural gas field, identified as Manifold South and Manifold North.
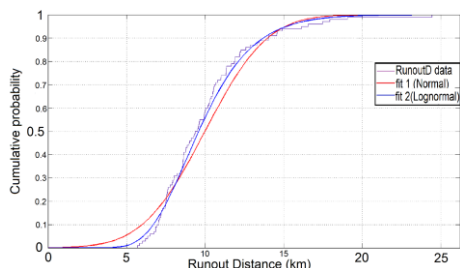

Figure 3. Runout distance cumulative distribution function along the natural channel.

Manifold South and Manifold North are located along the natural channel, respectively 10.5 km and 14.0 km from the crown of the slope under investigation (Figure 2). Therefore the probability of been impacted by the mud flow, given that the slope has failed, for the Manifold South and Manifold North are estimated using Eq. (4).

$$P_{impact} = P(Runout\ Distance \geq Manifold\ Location) \quad (4)$$

The conditional impact probabilities (given that slope failure has occurred) for the Manifold South and Manifold North are $P_{impactMS} = 0.37$ and $P_{impactMN} = 0.09$ respectively. These probabilities are based on the lognormal probability distribution function that best fits the numerical runout distance data.

5. Consequences

In this study the quantification of the direct consequences focused mainly on the cost of offshore equipment rather than the economic losses due to production disruption, and environment impact. It should be noted that the economic losses due to production disruption and environment impact are likely to be greater than the cost of the equipment, but their estimation requires complex analytical scenarios that are beyond the scope of this paper.

5.1. Elements at Risk

The offshore natural gas field is planned to be developed by deploying a system of seven wells and two manifolds (Figure 2). Manifold South will have four wells connected around it, and Manifold North will have three wells connected around it.

In this analysis it was considered that the critical offshore structures exposed to mud flow impact hazard are the manifolds. A production manifold is a subsea structure containing valves and pipework designed to combine and direct produced fluids from multiple wells into one or more flowlines. It is assumed that the pipelines that transport the produced natural gas to onshore facilities for further distribution follow a safe route away from the mud flow impact critical zone. The same applies for the subsea umbilicals, which are the link between topside and subsea systems by a series of cables and pipes that provide power and control to the subsea systems.

5.2. Vulnerability Curves

To estimate the consequences, the vulnerability curves for each element at risk are required. The estimated vulnerability (fragility) curves for the manifolds are based on the lateral capacity of their foundation. The foundation solution of the manifolds are suction caissons with nearly 6 m diameter and about 17 m length.

The maximum lateral capacity of the suction pile that may resist the mud flow impact forces is about 650 kN. The mud flow impact forces were examined through the work done by Zakeri (2008). The fluid dynamics approach proposed by Pfeiff and Hopfinger (1986) was applied.

This formulation is based on the classic fluid dynamics approach regarding the force experienced by an object moving through a fluid at relatively large velocity (i.e. high Reynolds number, Re >~1000). The drag coefficient is a function of the Reynolds number (i.e. Re = Inertial Forces/Viscous Forces) as well as the shape and surface rugosity of the object.

In this study it is assumed that the mud flow will impact the top part of the suction pile, at the interface between the suction pile and the manifold. Hence the impacted object was considered to have a cylinder shape with a smooth surface. The manifold itself is a very complex steel structure and it is difficult to estimate the drag coefficient based on its shape and surface rugosity.

The estimated vulnerability curves for the manifolds shown in Figure 4 are functions of the velocity and thickness of the mud flow.
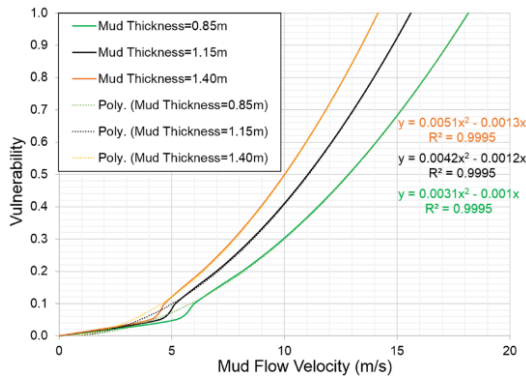

Figure 4. Vulnerability curves for exposed manifolds based on the velocity and thickness of the mud flow.

Table 2 shows the expected front velocity and thickness of the mud flow at 10.5 km (position of Manifold South) and 14.0 km (position of Manifold North) from the crown of the slope respectively. The values listed in Table 2 are based on probabilistic analyses of the simulation output data.

Table 2. Expected front velocity and thickness of mud flow

Distance from the Crown of the Slope (km)	Front Velocity (m/s)	Mud Thickness (m)
10.5	23	1.15
14.0	21	0.85

6. Risk Analysis

To estimate the risk associated to earthquake-induced submarine slope failure for the planned deep water natural gas development in the Gulf of Mexico, the classic definition of risk was applied (i.e. Risk= Hazard × Consequences).

In this context, *Hazard* can be defined as the annual probability of sediments impacting offshore structures given that a submarine slope failed, and can be estimated with Eq. (5).

P[Sediments impacting seabed installation] = P[EQ induced slope failure] × P[Sediments reaching seabed installation | Submarine slope has failed] (5)

Based on the information given in previous sections, the earthquake-induced slope failure risk analysis in the case study can be assessed by using the estimated unconditional annual probability of the earthquake-induced slope failure (i.e. UAFP = $1.2 \cdot 10^{-3}$) in section 3, and Eq. (5) as follows:

- Manifold South
  Using Eq. (5) to estimate the hazard:
  P[Sediments impacting Manifold South] = [$1.2 \cdot 10^{-3}$] × [0.37]= $4.4 \cdot 10^{-4}$
- Manifold North
  Using Eq. (5) to estimate the hazard:
  P[Sediments impacting Manifold North] = [$1.2 \cdot 10^{-3}$] × [0.09]= $1.1 \cdot 10^{-4}$

From the vulnerability curves shown in Figure 4 and Table 2, the estimated vulnerability for Manifold South and Manifold North is 1. Therefore the consequences can be estimated as follows:

Consequences = Manifold South (\$) × 1= Manifold South (\$).
Consequences = Manifold North (\$) × 1= Manifold North (\$).

It is noted that in this analysis the elements at risk have different hazard value given that they are located at different distances along the natural channel. The total risk for the elements at risk in this study can be estimated with Eq. (6).

$$Risk = \sum_{1}^{n} Hazard_n \times Consequences_n$$ (6)

Using Eq. (6) and assuming that the cost of Manifold South and Manifold North are the same, the total risk is $(4.4 + 1.1) \cdot 10^{-4} \times Manifold(\$) = 5.5 \cdot 10^{-4} \times Manifold(\$)$.

In other words, the annual risk associated to the earthquake-induced submarine slope failure for the future deep water gas development in the Gulf of Mexico is equal to the cost of the Manifold multiplied by $5.5 \cdot 10^{-4}$.

7. Discussion and Conclusions

This paper presented an offshore risk analysis for the planned deep water natural gas development in the Gulf of Mexico. It is focused on the direct consequences rather than the indirect consequences, specifically the potential damage to two planned Manifolds for collecting and transporting the hydrocarbons onshore.

To simulate the dynamics of the mud flow downslope, the 1-D numerical model BING developed by Imran (2001a) was used. However, BING does not account for the transport of sediments along channel surface configurations, which usually induce larger runout distances and debris flow velocities due to the increase of inertial forces and thickness of the shear layer compared to non-channel surface configurations. On the other hand, the BING model does not account for the resistance generated at the interface between the moving debris and the ambient fluid above, which may result in overestimated runout distances and velocities of the debris flows, as Rodríguez-Ochoa et al. (2015a) showed. The latter limitation may counterbalance the absence of the channel effect during the debris flow numerical simulations.

This work presents all the required steps to carry out the risk analysis in a systematic manner, including:

1. Estimation of the annual probability of earthquake-induced slope failure;
2. Identification of the elements at risk;
3. Probability of impacting seabed installations (elements at risk) given that the submarine slope already failed;
4. Estimation of vulnerability curves for the elements at risk to assess the consequences; and
5. Evaluation of the risk.

To estimate the annual probability of earthquake-induced slope failure, the slope failure fragility curve approach proposed by Rodríguez-Ochoa et al. (2015b) was used. The probability of impacting a seabed installation given that the submarine slope already failed, was obtained by numerical simulation of debris flows in BING code (Imran, 2001) and Monte Carlo method.

The annual risk associated to the failure of submarine slope was found to be about 0.0005 times the cost of the Manifold ($).

References

Fugro, GeoConsulting. (2009). *Investigación Geológica y Geotécnica Integrada, Sonda de Campeche, México.*

Geomatrix. 2006. *Evaluación de Peligrosidad Sísmica, Bahía de Campeche, México.*

Imran, J., Harff, P., Parker, G. (2001a). A numerical model of submarine debris flow with graphical user interface, *Computers and Geosciences* **27** (6), 717–729.

Imran, J., Parker, G., Locat, J., Lee, H. (2001b). 1D Numerical Model of Muddy Subaqueous and Subaerial Debris Flows, *Journal of Hydraulic Engineering* **127** (11), 959–968.

Jeong, S.W., Locat, J., Leroueil, S., Malet, JP. (2010). Rheological properties of fine-grained sediment: the roles of texture and mineralogy, *Canadian Geotechnical Journal* **47** (10), 1085–1100.

Locat, J. (1997). Normalized rheological behaviour of fine muds and their flow properties in a pseudoplastic regime, *Debris-flow hazard mitigation: mechanics, prediction, and assessment.* Chen et.al. (eds.), 260–269, San Francisco California, USA, 7-9 August 1997.

McKay, M.D., Beckman, RJ., Conover, WJ. (2000). A Comparison of Three Methods for Selecting Values of Input Variables in the Analysis of Output from a Computer Code, *Technometrics* **42**, 55–61.

Nadim, F. (2012). Risk Assessment for Earthquake-Induced Submarine Slides, *Submarine Mass Movements and Their Consequences*, Yamada et.al. (eds.), 15–27, Kyoto, Japan, 24-26 October 2011.

Pfeiff, C.F., Hopfinger, EJ. (1986). Drag on Cylinders Moving Through Suspensions With High Solid Concentration, *PCH PhysicoChemical Hydrodynamics,* **7** (2), 101–109.

Rodríguez-Ochoa, R., Nadim, F., Cepeda, JM. (2015a). Correction Factors for 1-D Runout Analyses of Selected Submarine Slides, *Submarine Mass Movements and Their Consequences*, (accepted), Wellington, New Zealand, 1-4 November 2015.

Rodríguez-Ochoa, R., Nadim, F., Cepeda, JM., Hicks, MA., Liu, Z. (2015b). Hazard analysis of seismic submarine slope instability, *Georisk* (accepted).

Rodríguez-Ochoa, R., Nadim, F., Hicks, MA. (2015c). Influence of Weak Layers on Seismic Stability of Submarine Slopes, *Marine and Petroleum Geology* **65** 247-268.

Zakeri, A. (2008). *Submarine Debris Flow Impact on Pipelines*, University of Oslo, Oslo, Norway, ISSN 1501-7710.